Lecture Notes

Introduction to Strongly Correlated Electron Systems

WS 2014/ 2015

Mohsen Abd-Elmeguid

II. Institute of Physics, University of Cologne, Germany

Introduction to strongly correlated electron systems

I. Introduction

Brief summary of electrons in solids, origin of strong electron correlations

II. Classes of strongly correlated electron systems

(a) Transition metal compounds: 3d-electrons

- Hubbard model, Mott insulator, metal-insulator transition
- Spin, charge, and orbital degrees of freedom and ordering phenomena, selected materials

(b) Heavy fermion systems: 4f (5f) – electrons

- The Kondo effect, heavy fermion systems, non-Fermi liquid behavior,
- Quantum phase transitions, unconventional superconductivity, selected materials

(c) Nanoscale structures:

- Quantum confinement, unusual properties for potential applications

III. Pressure effect on the ground state properties:

- Recent experimental results on heavy fermions and transition metal compounds

IV. Summary and open discussion

selected materials

Doped Mott insulators

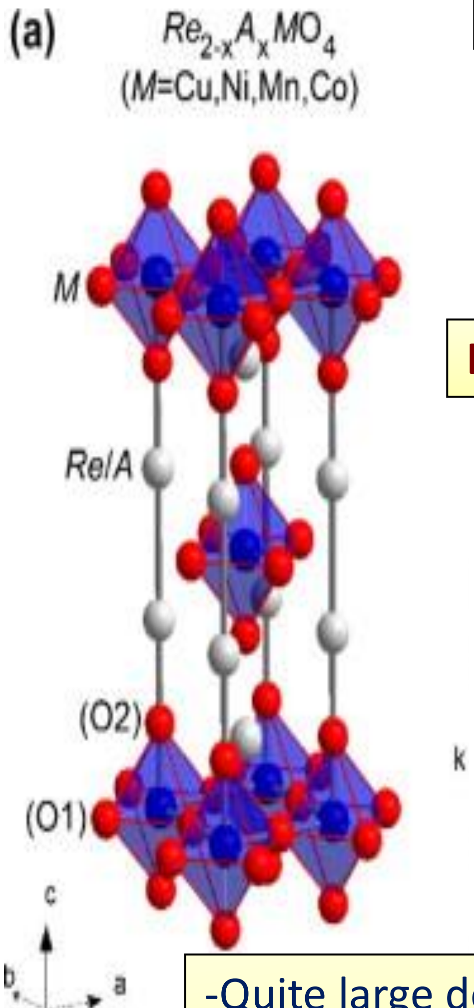

Example: (Re,A)2MO4

Layered structure ⟹ quasi-2D system ⟹ MO2-planes

Re: La3+, A: Sr2+, M: Cu,Ni,Mn,Co

⇓

Hole doping

-Quite large doping required to overcome charge/spin/orbital Long range order

-Doped carriers can self assemble ⟹ some examples!

H. Ulbrich, M. Braden / Physica C 481 (2012) 31–45

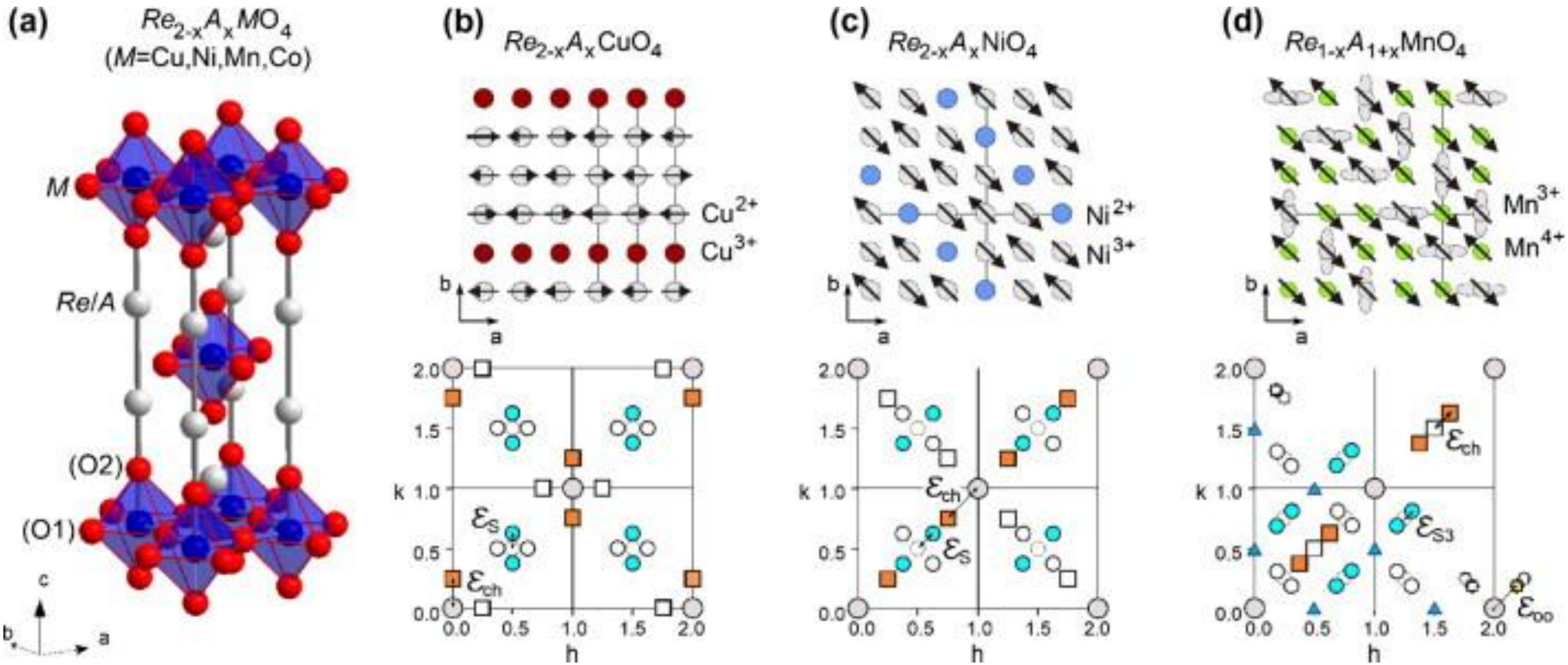

In the cuprates with large doping, charges are found to segregate in stripes running along the Cu–O bonds and are therefore called horizontal (or vertical) stripes. In the nickelates stripes are observed to run along the diagonals (diagonal stripes) as it is also reported for low-doped $La_{2-x}Sr_xCuO_4$

Getting control of the properties in TMO systems

correlation physics here has an energy scale of eV

but decision between metallic vs. insulator, FM vs. AFM is on much lower energy scale!

⇓

tiny perturbations of the system lead to a huge change of the properties

Giant Magnetoresistance (CMR)

Experimentally Driven 1986-1989; Theoretically Modeled 1989; IT Applications into 1990's

First Commerical Hard-Disks with GMR Sensors (IBM) 1998

1988: … simultaneously, but independent

Nobel Prize in Physics 2007

Albert Fert

Peter Grünberg

Giant magnetoresistance (GMR)

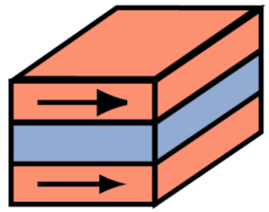

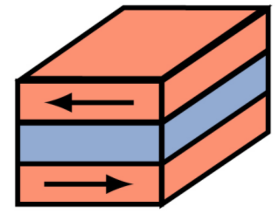

Ferromagnet
Metal
Ferromagnet

Electrical resistance: R_P R_{AP}

The electrical resistance depends on the relative magnetic alignment of the ferromagnetic layers

$$\mathrm{GMR} = \frac{R_{AP} - R_P}{R_P}$$

19% for trilayers @RT

80% for multilayers @ RT

- only occurs for thin spacers with a thickness of a few nm
- observed for many metallic spacer layers

GMR is much larger than the anisotropic magnetoresistance (AMR)

First observations of GMR

Both experiments employ antiferromagnetic interlayer coupling to achieve the antiparallel alignment

P. Grünberg, FZJ [1]

(a) Fe/Cr/Fe trilayer: 1.5% @ 300 K

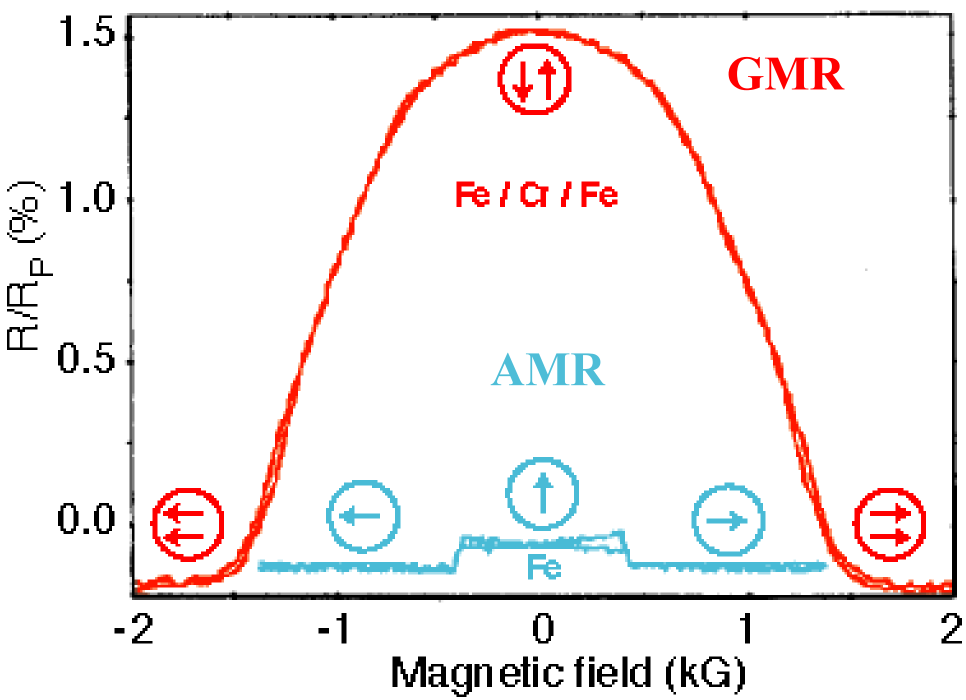

A. Fert, Paris-Sud [2]

(b) Fe/Cr multilayers: 80% @ 4.2 K

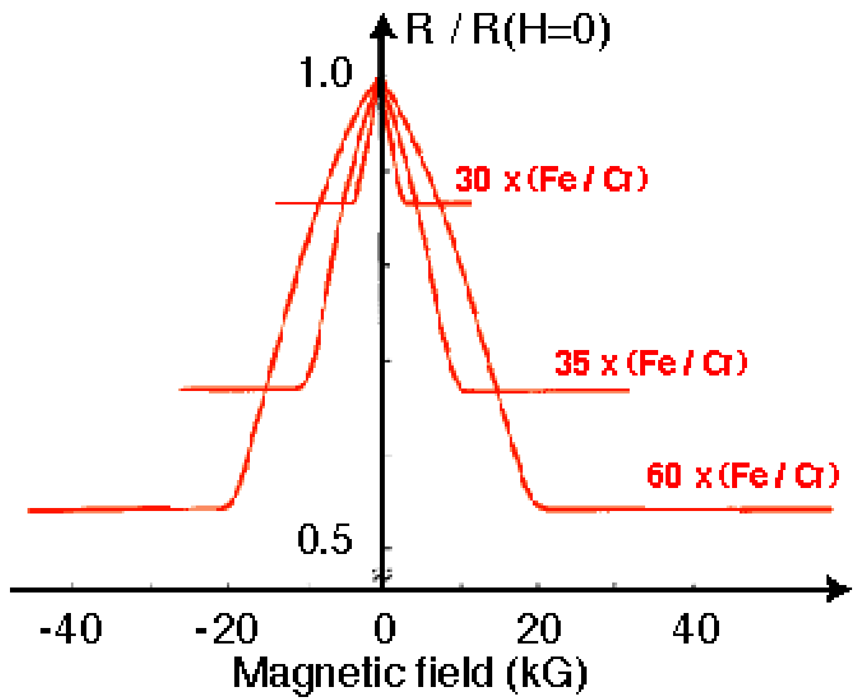

[1] G. Binasch, P. Grünberg *et al.,* Phys. Rev B 39, 4828 (1989)

[2] M.N. Baibich, A. Fert *et al.*, Phys. Rev. Lett. 61, 2472 (1988)

Anisotropic Magnetoresistance (**AMR)**

Spontaneous resistivity anisotropy ratio generally defined as

$$SRA = \frac{\Delta\rho}{\bar{\rho}} \qquad\qquad SRA = \frac{\rho_{\parallel} - \rho_{\perp}}{\rho_{\parallel}/3 + 2\rho_{\perp}/3}$$

- **Origin:** spin-orbit interaction -> coupling adds some orbital contribution to the spin moment, gives rise to a dependence of the electron scattering on the angle between the electron wave vector and the magnetization direction
- Effect disappears above T_c

For permalloy $Ni_{80}Fe_{20}$ $SRA \sim 4\%$

The largest AMR effect at room temperature is found for $Ni_{1-x}Co_x$ alloys with x close to 0.2, for which $SRA \sim 6\%$

First observations of GMR

Both experiments employ antiferromagnetic interlayer coupling to achieve the antiparallel alignment

P. Grünberg, FZJ [1]

A. Fert, Paris-Sud [2]

(a) Fe/Cr/Fe trilayer: 1.5% @ 300 K

(b) Fe/Cr multilayers: 80% @ 4.2 K

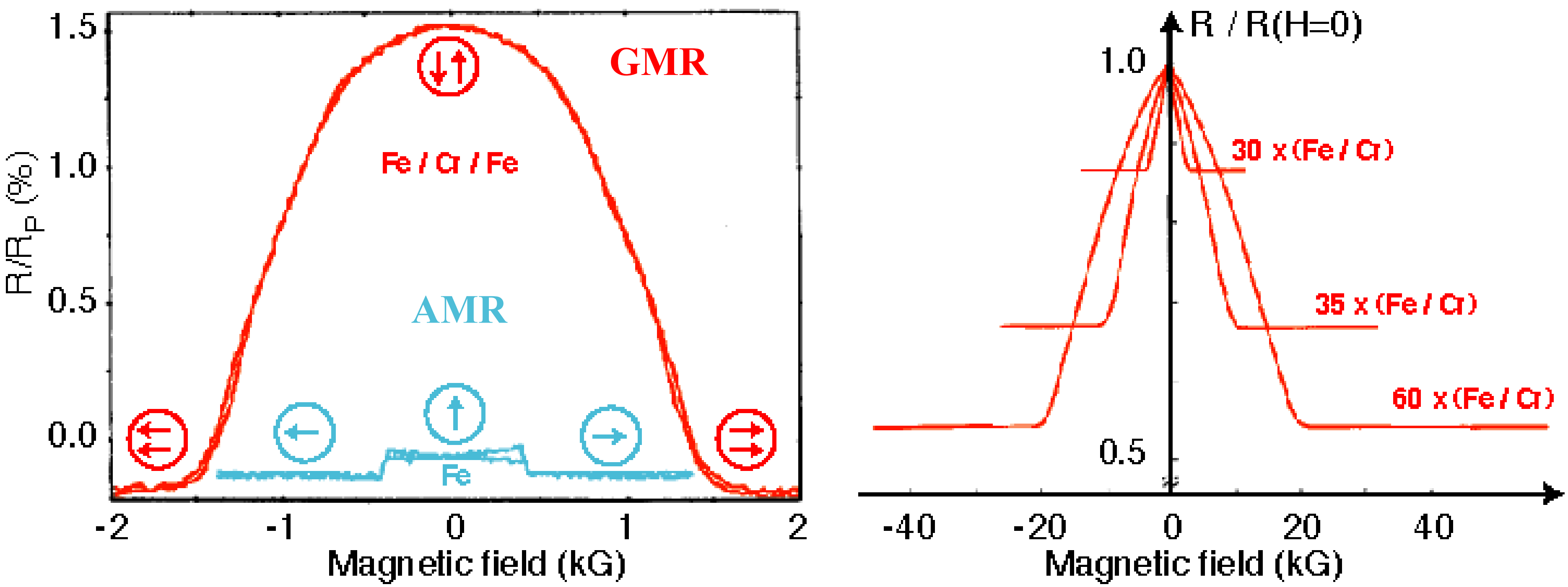

[1] G. Binasch, P. Grünberg *et al.,* Phys. Rev B 39, 4828 (1989)

[2] M.N. Baibich, A. Fert *et al.*, Phys. Rev. Lett. 61, 2472 (1988)

Clossal Magnetoresistance in doped TMO (CMR)

Example:

The Ca-doped series : $La_{1-x}Ca_xMnO_3$

Doped manganites

Perovskite structure

$A_{1-x} B_x \mathrm{MnO_3}$

A = trivalent alkaline ion

B = divalent rare earth

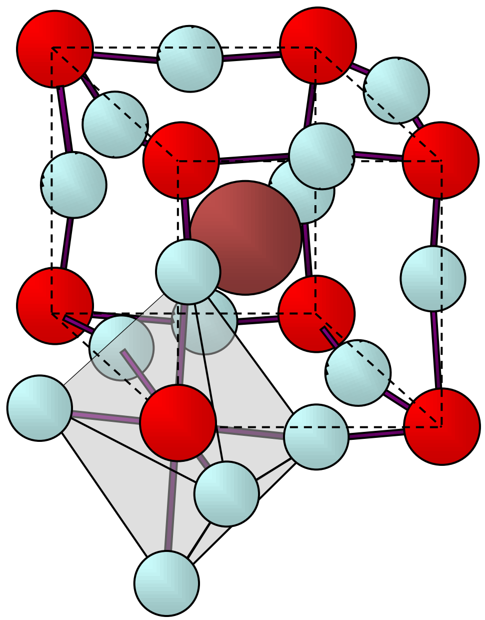

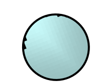
O^{2-}

Mn mixed valence :

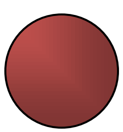 $A = La^{3+}, Y^{3+}$… ⟺ 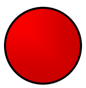 Mn^{3+}

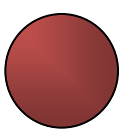 $B = Sr^{2+}, Ca^{2+}$… ⟺ 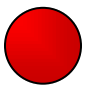 Mn^{4+}

The Ca-doped series : $La_{1-x}Ca_xMnO_3$

- La^{3+} and Ca^{2+} are subsitutional
- $La_{1-x}Ca_xMnO_3$ solid solution can be obtained with $0 \leq x \leq 1$:

$LaMnO_3$ $\xrightarrow{x_{Ca}}$ $CaMnO_3$

Mn^{3+} — Mn^{4+}

Jahn-Teller active ion — Non Jahn-Teller active

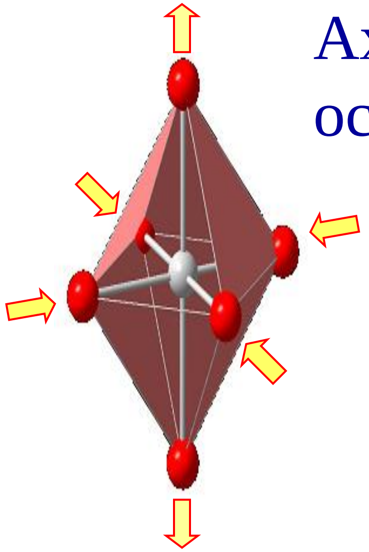

Axially elongated octahedron

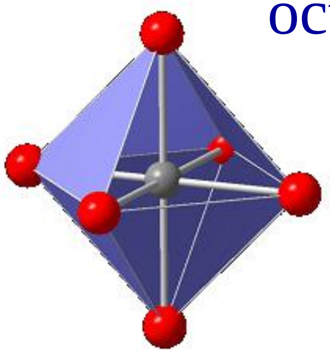

Regular octahedron

Temperature *vs* doping phase diagram

Doped manganites have complex phase diagram

FM = FerroMagnetic

AF = AntiFerromagnetic

CAF = Canted AF

FI = FM Insulator

CO = Charge Ordered

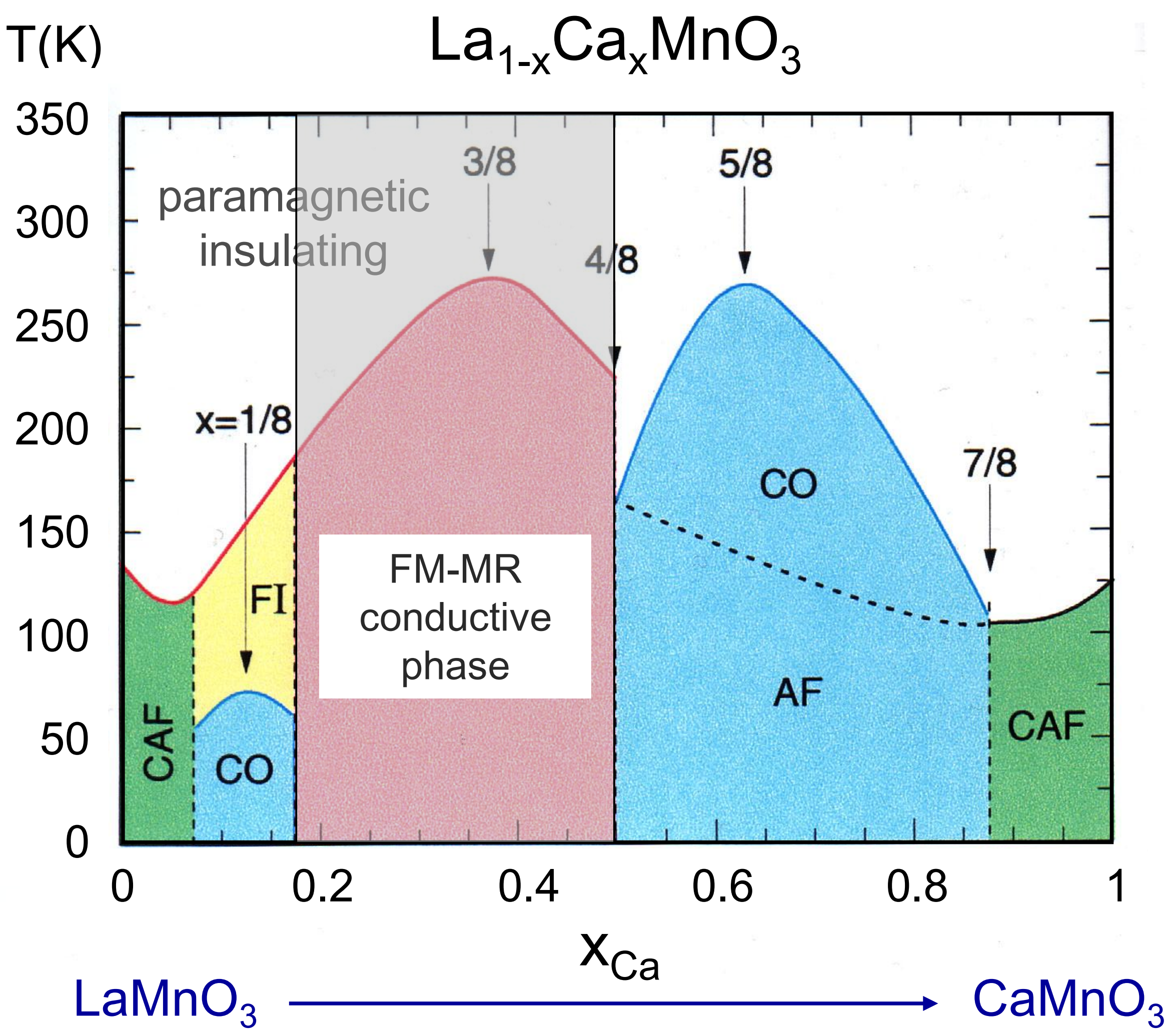

Maximum MR at x = 0.25

magneto-transport properties

Magnetic

transition (T_C)

⇕

Metal-to-Insulator

transition (T_{MI})

⇕

Structural

transition (T_S)

($T_C \sim T_{MI} \sim T_S$)

<u>Local</u> structure :

- Mn-O bond lengths
- Mn-O-Mn bond angles

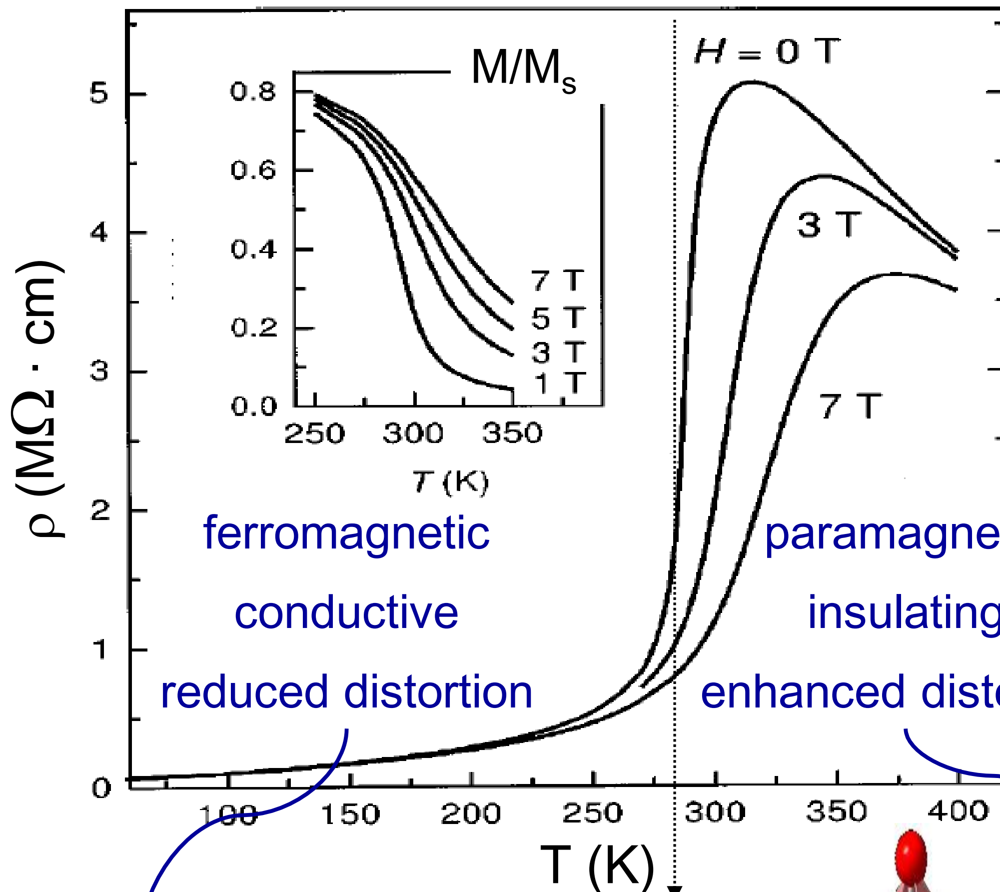

$T_C \sim 260$ K

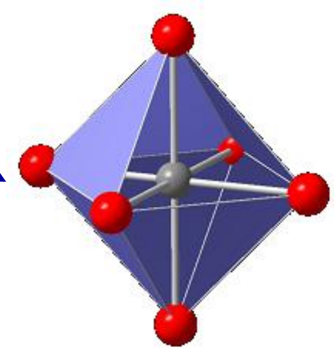

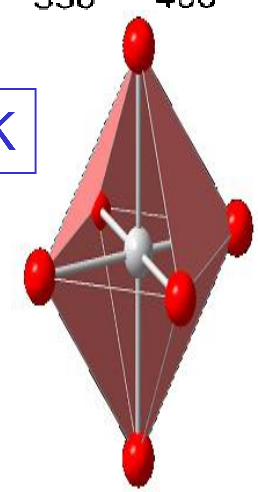

CMR (colossal magnetoresistance) $La_{0.75}Ca_{0.25}MnO_3$

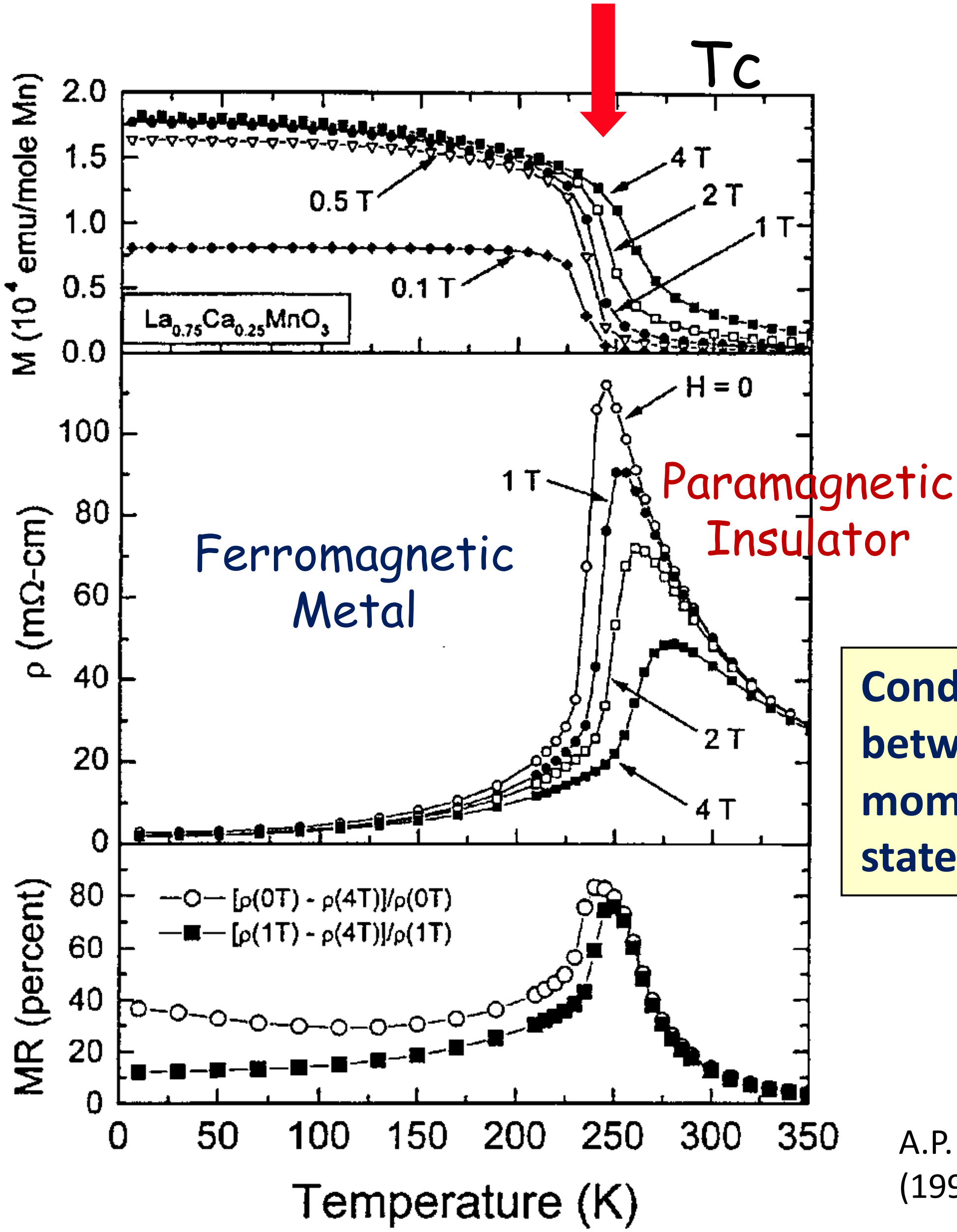

Magnetoresistance is defined as the relative change of resistances at different magnetic fields

$$\Delta R = \frac{R(H=0) - R(H)}{R(H)}$$

Conduction is by hopping of electrons between Mn3+ and Mn4+ sites, magnetic moments must be parallel ! → ferromagnetic state is needed

A.P. Ramirez, J. Phys.: Condens. Matter., 9 (1997) 8171

correlated 4d and 5d transition metal oxides

Why interesting?

4d and 5d orbitals are more extended than 3d's

- reduced on-site Coulomb interaction strength
- sensitive to lattice distortion, magnetic order, etc.
- spin-orbit (SO) coupling much stronger! (mainly 5d comounds)

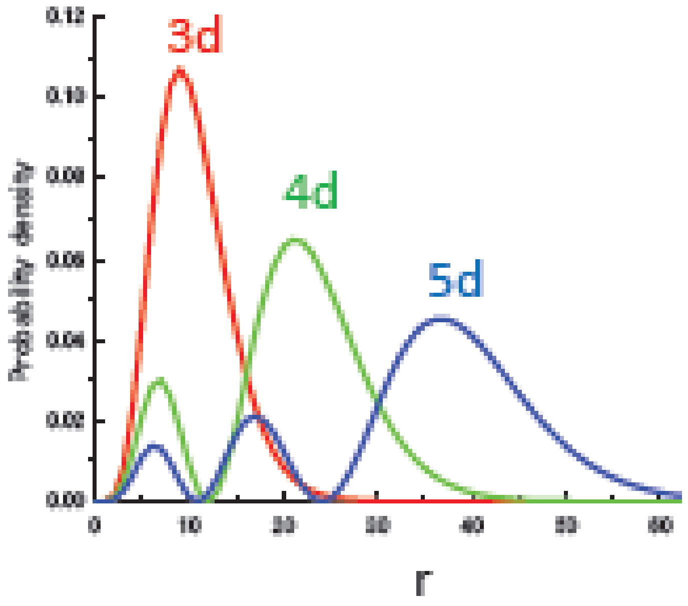

Examples!

3.2 Dzyaloshinskii-Moriya interaction

- 2D square lattice (***J**$_{eff}$*=1/2 moments) with large ***J***$_{SE}$
  - similar to undoped high-T$_C$ cuperates
- Dzyaloshinskii-Moriya interaction:

$$H_{DM} = \sum_{\langle i,j \rangle} \vec{D}_{ij} \cdot (\vec{S}_i \times \vec{S}_j); \quad | \vec{D}_{ij} | \propto \lambda; \quad \Rightarrow$$

favors **non-colinear** spin arrangement

$$\vec{D}_{ij} \propto \lambda \vec{x} \times \vec{r}_{ij}$$

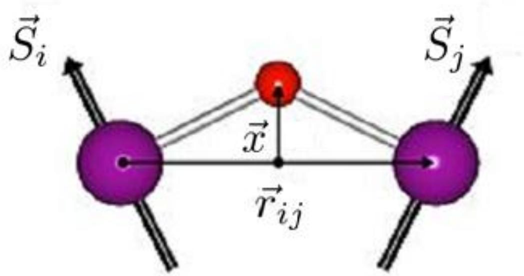

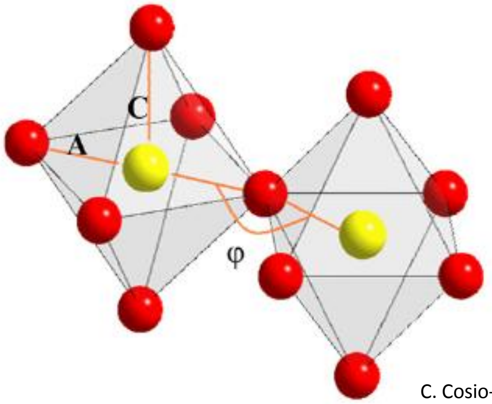

	Sr_2IrO_4
a-cell parameter (Å)	5.4921
c-cell parameter (Å)	25.7666
A (Å)	1.968
C (Å)	2.301
φ (deg)	161.37

C. Cosio-Castaneda et al. J. Phys.: Condens. Matter 19 (2007)

$$\varphi \neq 180^\circ \Rightarrow \vec{x} \neq \vec{0} \Rightarrow \vec{D}_{ij} \neq \vec{0}$$

Ruthenates

Ruddlesden-Popper (RP) series $(Sr,Ca)_{n+1}Ru_nO_{3n+1}$

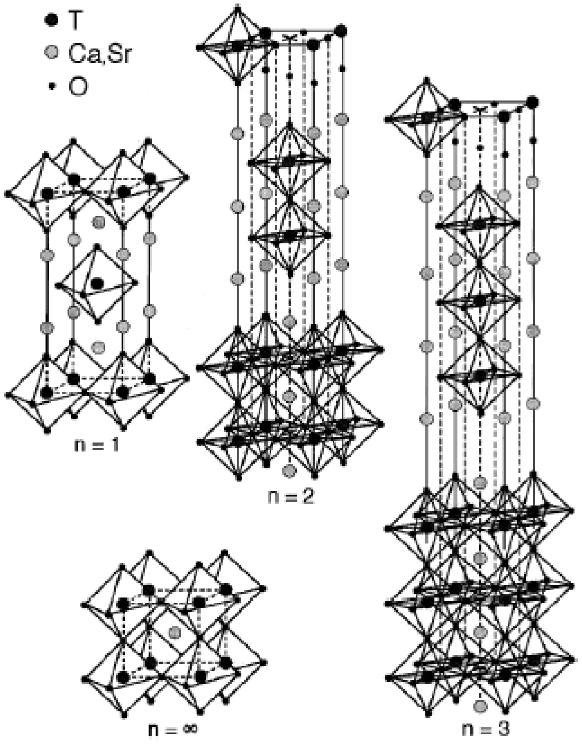

n=1,Sr_2RuO_4(SC),

Ca_2RuO_4(AF insulator);

n=2,$Sr_3Ru_2O_7$,$Ca_3Ru_2O_7$;

n=3,$Sr_4Ru_3O_{10}$

Crystal structures for various n. T site is Ru.

G. Cao *et al.* Matl. Sci. Eng. B **63**,76 (1999)

Ru electronic configuration: [Kr]$4d^7 5s^1$

Rutherate (Ru^{4+})

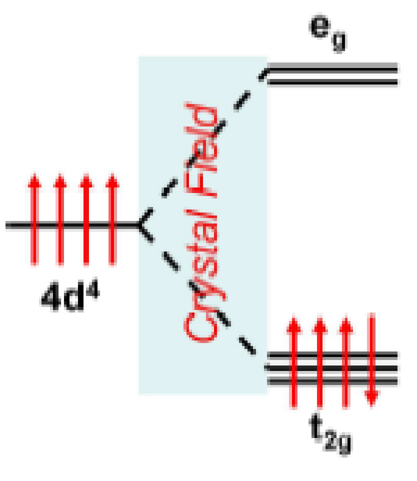

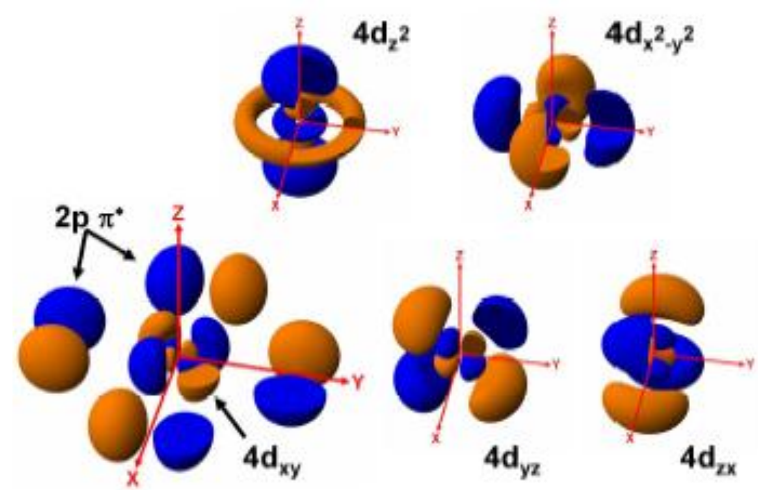

phase diagram of $Ca_{2-x}Sr_xRuO_4$

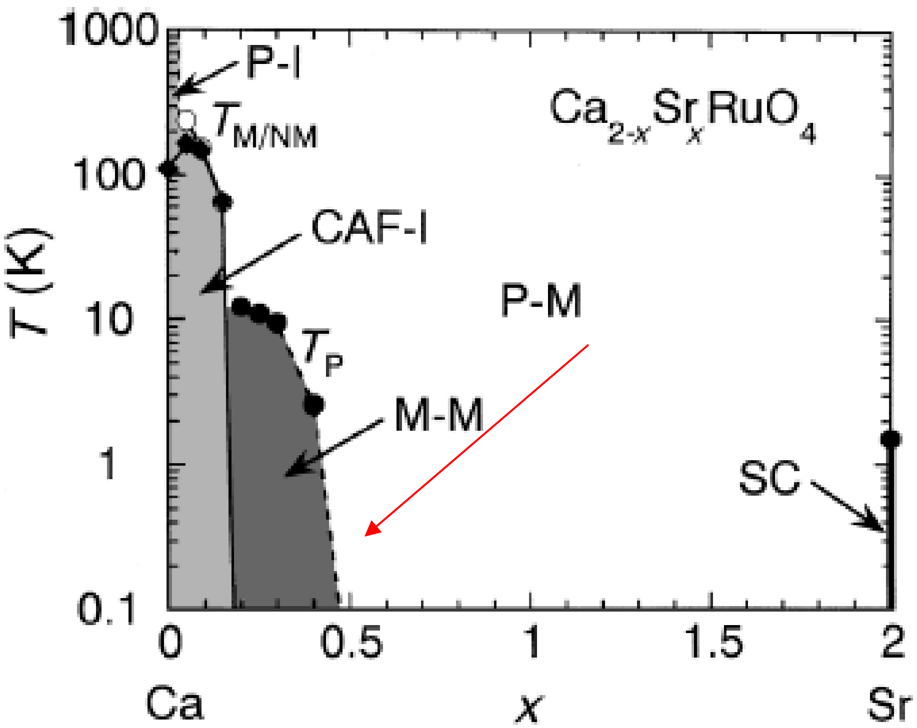

P: paramagnetic,
CAF: canted antiferromagnetic,
M: magnetic,
SC: superconducting,
-M: metallic phase,
–I : insulating phase.

(I) $(0 \leq x < 0.2)$ AF insulating ground state;

(II) $(0.2 \leq x < 0.5)$ Magnetic metallic (M-M) region;

(III) $(0.5 \leq x \leq 2)$ Paramagnetic metal.

S. Nakatsuji *et al* Phys. Rev. Lett. **84**, 2666 (2000)

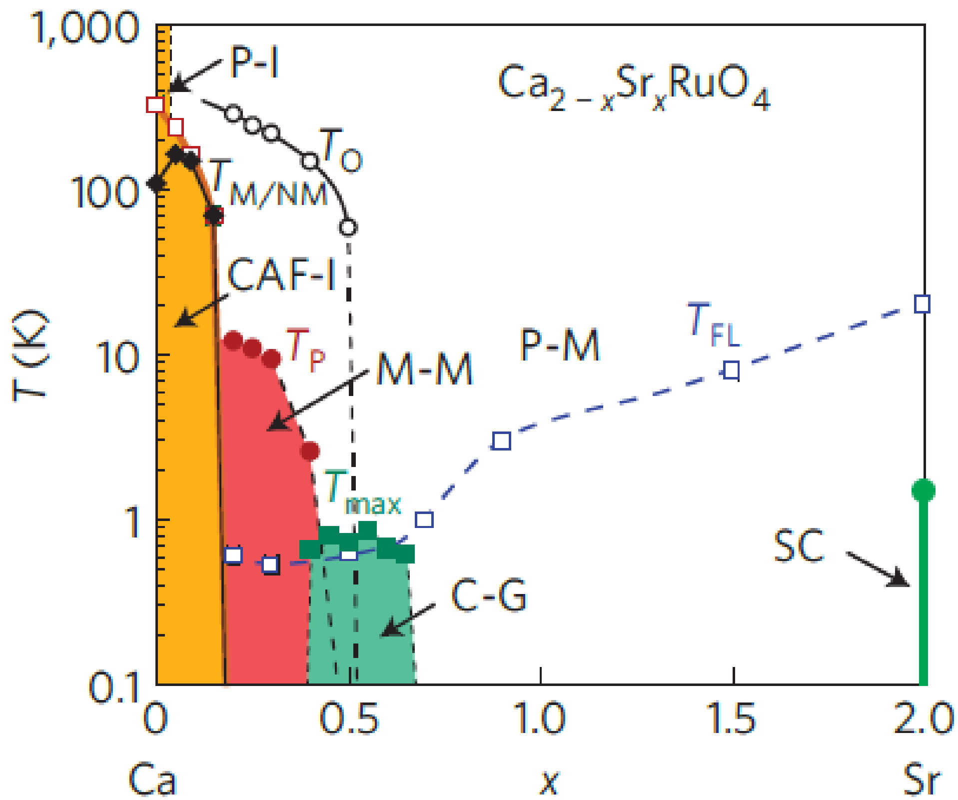

Nakatsuji, S. & Maeno, Y. Switching of magnetic coupling by a structural symmetry change near the Mott transition in $Ca_{2-x}Sr_xRuO_4$. *Phys. Rev. B* **62,** 6458–6466 (2000).

Nakatsuji, S. & Maeno, Y. Quasi-two-dimensional Mott transition system $Ca_{2-x}Sr_xRuO_4$. *Phys. Rev. Lett.* **84,** 2666–2669 (2000).

. Nakatsuji, S. *et al.* Heavy-mass Fermi liquid near a ferromagnetic instability in layered ruthenates. *Phys. Rev. Lett.* **90,** 137202 (2003).

Detailed structural studies (Braden s Group)

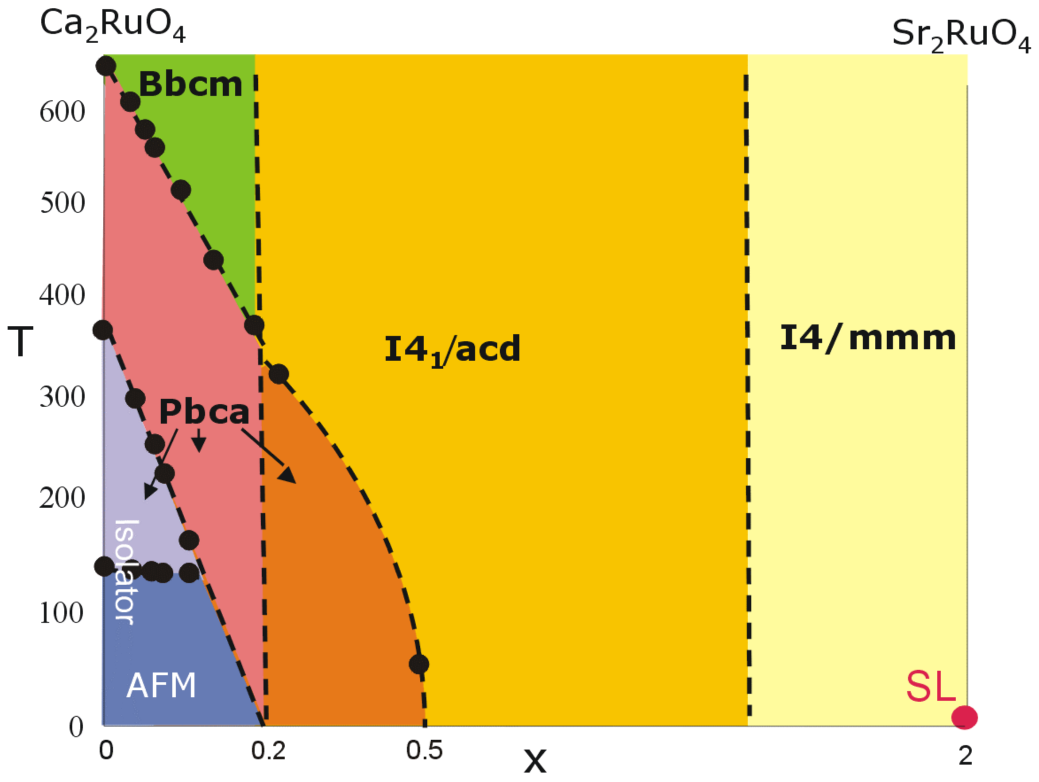

Steffens et al. PRB 72,094104 (2005).

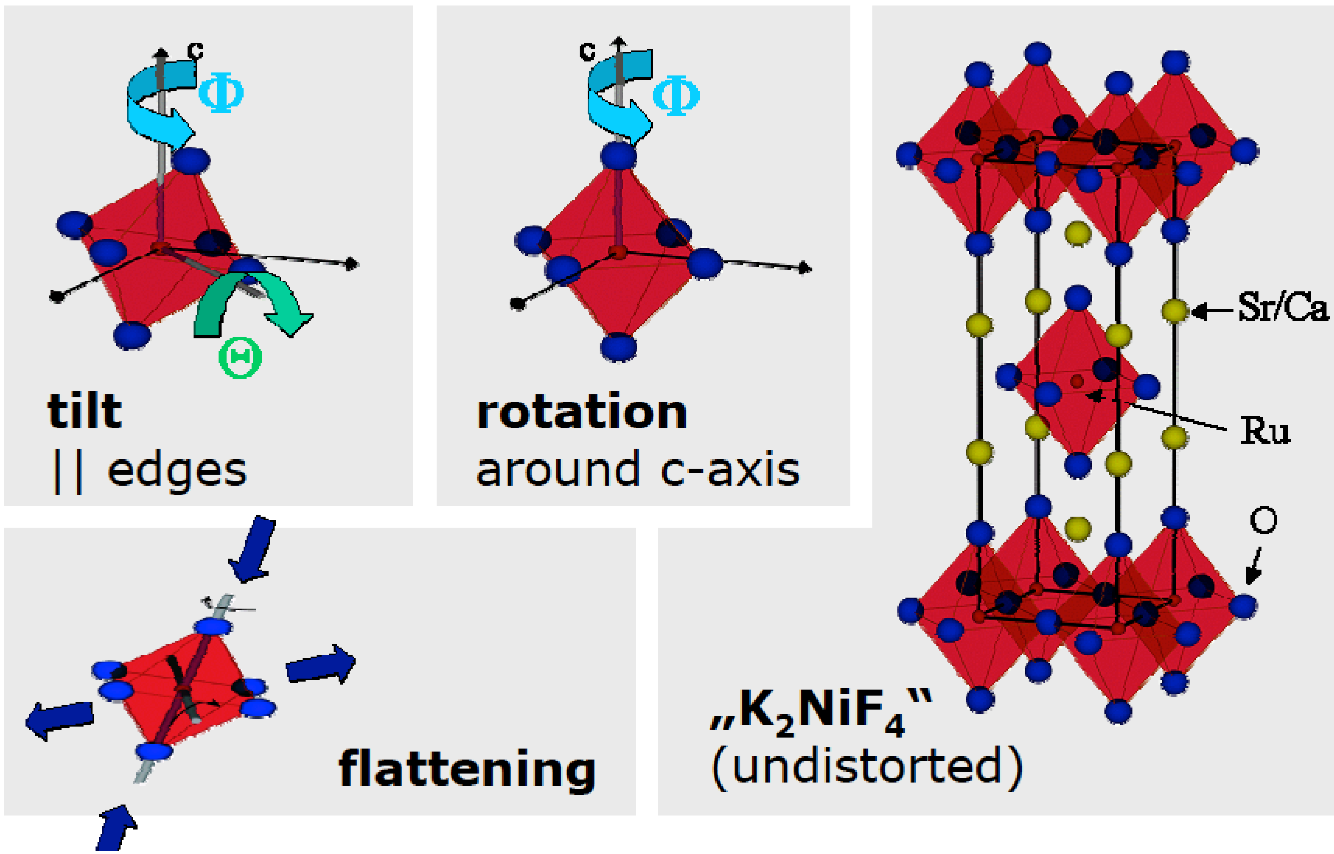

c
Φ
Θ
tilt
|| edges
c
Φ
rotation
around c-axis
flattening
Sr/Ca
Ru
O
„K2NiF4"
(undistorted)

NATURE MATERIALS | VOL 11 | APRIL 2012 |

New magnetic phase diagram of $(Sr,Ca)_2RuO_4$

J. P. Carlo[1,2], T. Goko[1,3], I. M. Gat-Malureanu[1,4], P. L. Russo[1], A. T. Savici[1], A. A. Aczel[5], G. J. MacDougall[5], J. A. Rodriguez[5], T. J. Williams[5], G. M. Luke[5], C. R. Wiebe[1,5], Y. Yoshida[6], S. Nakatsuji[7,8], Y. Maeno[7], T. Taniguchi[9] and Y. J. Uemura[1]*

High-T_c cuprates, iron pnictides, organic BEDT and TMTSF, alkali-doped C_{60}, and heavy-fermion systems have superconducting states adjacent to competing states exhibiting static antiferromagnetic or spin density wave order. This feature has promoted pictures for their superconducting pairing mediated by spin fluctuations. Sr_2RuO_4 is another unconventional superconductor which almost certainly has a p-wave pairing. The absence of known signatures of static magnetism in the Sr-rich side of the (Ca, Sr) substitution space, however, has led to a prevailing view that the superconducting state in Sr_2RuO_4 emerges from a surrounding Fermi-liquid metallic state. Using muon spin relaxation and magnetic susceptibility measurements, we demonstrate here that $(Sr,Ca)_2RuO_4$ has a ground state with static magnetic order over nearly the entire range of (Ca, Sr) substitution, with spin-glass behaviour in $Sr_{1.5}Ca_{0.5}RuO_4$ and $Ca_{1.5}Sr_{0.5}RuO_4$. The resulting new magnetic phase diagram establishes the proximity of superconductivity in Sr_2RuO_4 to competing static magnetic order.

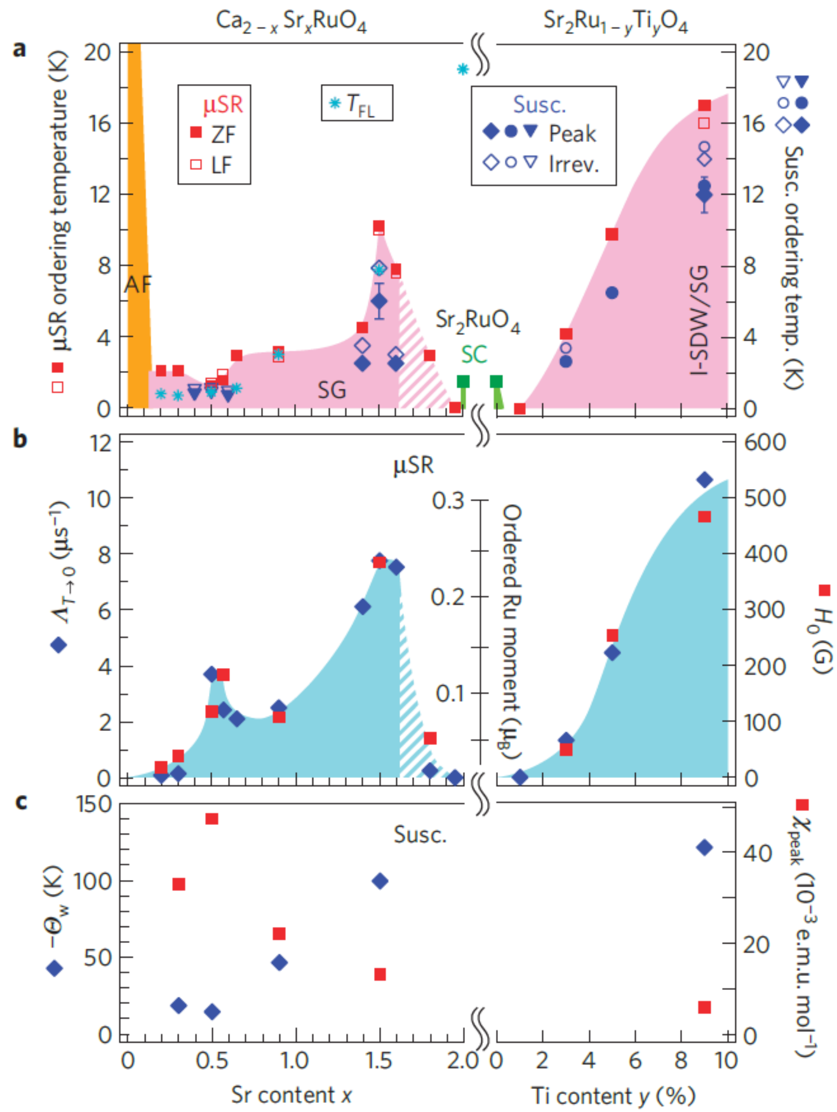
a
b
c
$Ca_{2-x}Sr_xRuO_4$
$Sr_2Ru_{1-y}Ti_yO_4$
μSR ordering temperature (K)
Susc. ordering temp. (K)
μSR
ZF
LF
T_{FL}
Susc.
Peak
Irrev.
AF
SG
Sr_2RuO_4
SC
I-SDW/SG
$\Lambda_{T\to0}$ (μs^{-1})
μSR
Ordered Ru moment (μ_B)
H_0 (G)
$-\Theta_w$ (K)
Susc.
χ_{peak} (10^{-3} e.m.u. mol^{-1})
Sr content x
Ti content y (%)

Continuous research activities in Cologne

PHYSICAL REVIEW B **89**, 045119 (2014)

Spin-density-wave ordering in $Ca_{0.5}Sr_{1.5}RuO_4$ studied by neutron scattering

S. Kunkemöller,[1] A. A. Nugroho,[2] Y. Sidis,[3] and M. Braden[1,*]
[1]*II. Physikalisches Institut, Universität zu Köln, Zülpicher Straße 77, D-50937 Köln, Germany*
[2]*Faculty of Mathematics and Natural Sciences, Institut Teknologi Bandung, Jalan Ganesha 10, 40132 Bandung, Indonesia*
[3]*Laboratoire Léon Brillouin, CEA/CNRS, F-91191 Gif-sur-Yvette Cedex, France*
(Received 6 December 2013; published 14 January 2014)

correlated 4d and 5d transition metal oxides

Why interesting?

4d and 5d orbitals are more extended than 3d's

- reduced on-site Coulomb interaction strength
-sensitive to lattice distortion, magnetic order

- spin-orbit (SO) coupling much stronger! (mainly 5d compounds)

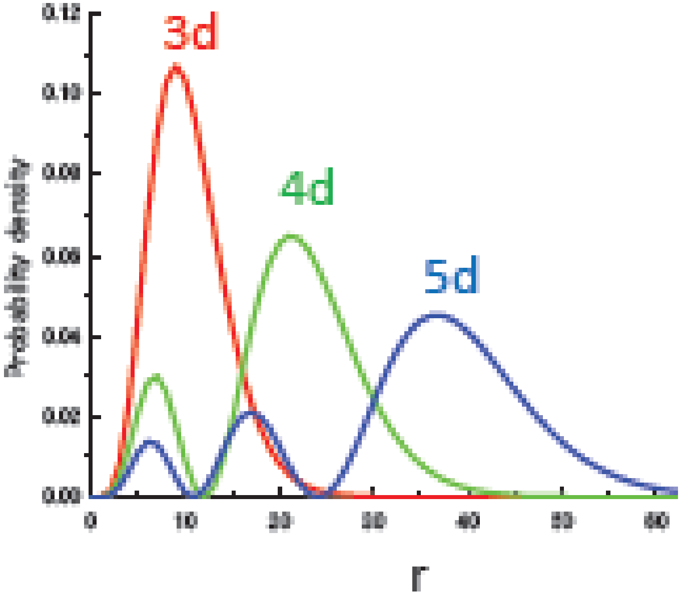

Example: **SO-assisted Mott transition** in Sr_2IrO_4

spin-orbit coupling

- interaction of angular momentum around nucleus ***L*** and spin ***S*** of electron:

$$\zeta_{SO} = \frac{\lambda}{\hbar^2}\vec{L}\cdot\vec{S}$$

$$\zeta_{SO} = \frac{\lambda}{2}(j(j+1) - l(l+1) - s(s+1))$$

- ➢ total angular moment: $\vec{J} = \vec{L} + \vec{S}$
- ➢ coupling strength:

$$\lambda = \frac{Ze^2\mu_0\hbar^2}{8\pi m_e^2 r^3}; \quad r \propto \frac{1}{Z} \Rightarrow \boxed{\lambda \propto Z^4}$$

spin-orbit coupling

SO-coupling is a fast growing effect:

Z:	25	29	44	77	80
TM:	Mn	Cu	Ru	Ir	Hg
λ:	1/2	1	2	50	58

$\lambda_{Ir} \approx 25\lambda_{Rh}$

$\zeta_{SO} \approx 0,4 - 0,5 eV$

Systems with correlation + strong SO coupling

extended 5d orbitals → reduced Coulomb repulsion ***U*** (***U***~ ***W***).
strength of **SO** coupling ***λ*** and ***U*** become comparable.

Hubbard model with strong SO coupling (mean-field):

$$\mathcal{H} = \sum_{i,j,\alpha,\beta,\sigma} t_{ij,\alpha\beta}\, c^{\dagger}_{i\alpha} c_{j\beta} + \lambda \sum_{i} \vec{L}_i \cdot \vec{S}_i + U \sum_{i,\alpha} n_{i\alpha\uparrow} n_{i\alpha\downarrow}$$

↑ kinetic energy: electron hops from j to i

spin-orbit coupling

↑ Considering only one orbital (α)

sites i, j, orbitals α, β, spin σ

Systems with correlation + strong SO coupling

Spin-Orbit- assisted Mott insulators: SrIr2O4

Sr_2IrO_4

$5d^5$ transition metal oxide

B.J. Kim et al. Science 323 (2009)

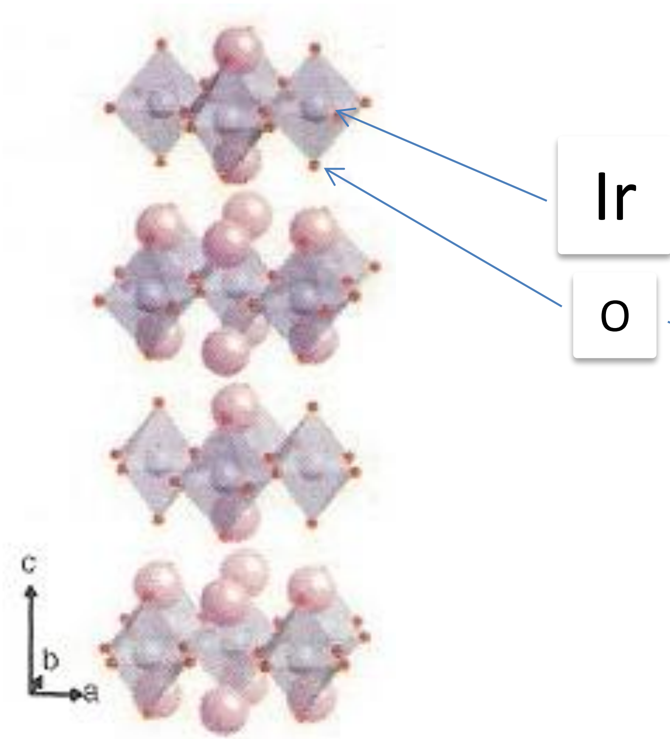

K2NiF4-structure

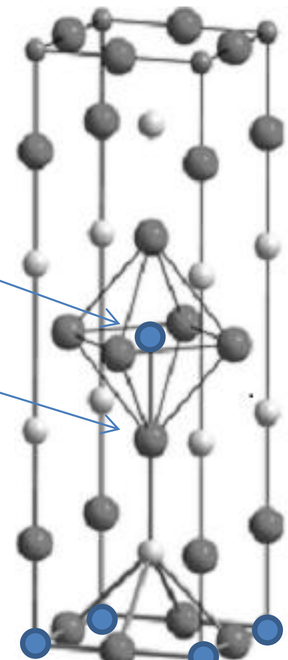

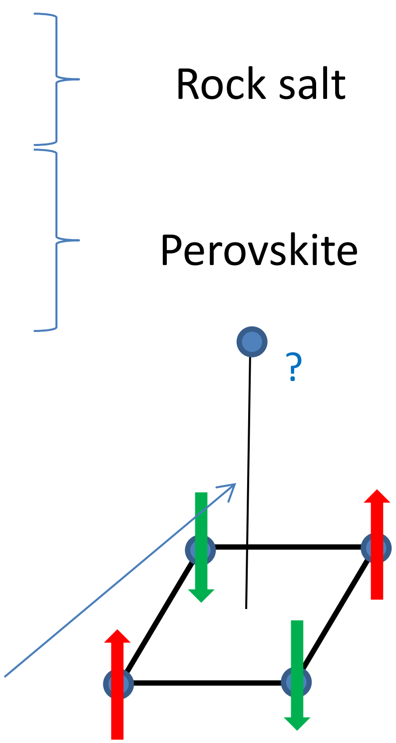

magnetic frustration
along c-axis

Sr_2IrO_4

expected behavior using LDA

metallic ground state

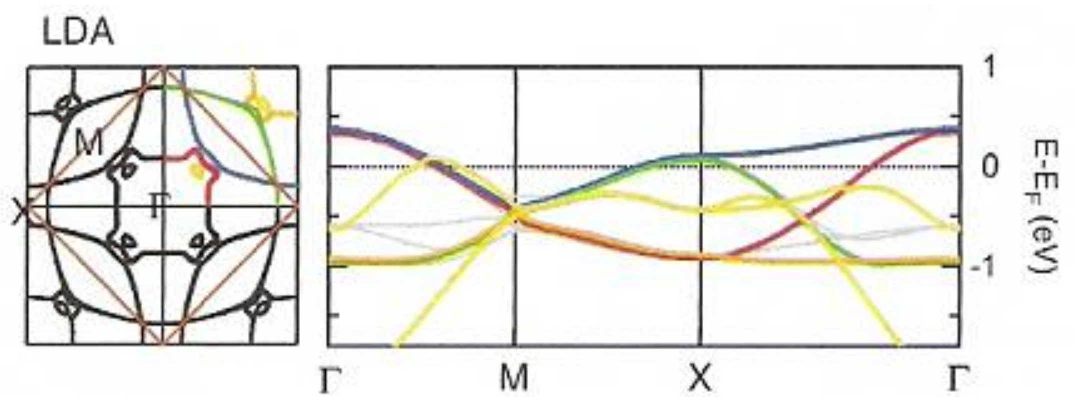

- Similar to $Sr_2^{2+}Rh^{4+}O_4^{2-}$:
  - $4d^5$ TMO with metallic ground state

observed behavior

insulating ground state

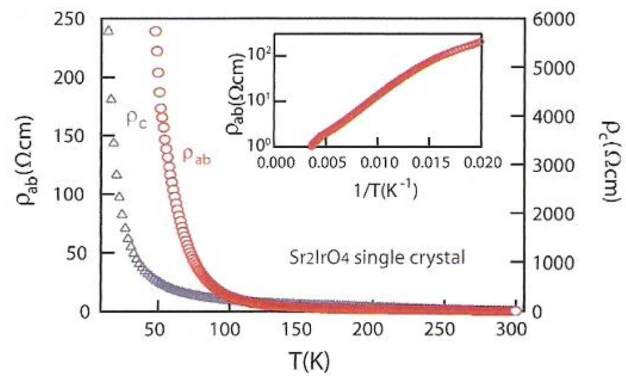

weak ferromagnetism

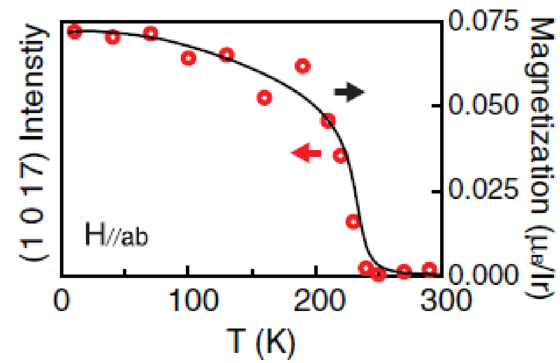

B.J. Kim et al. Science 323 (2009)

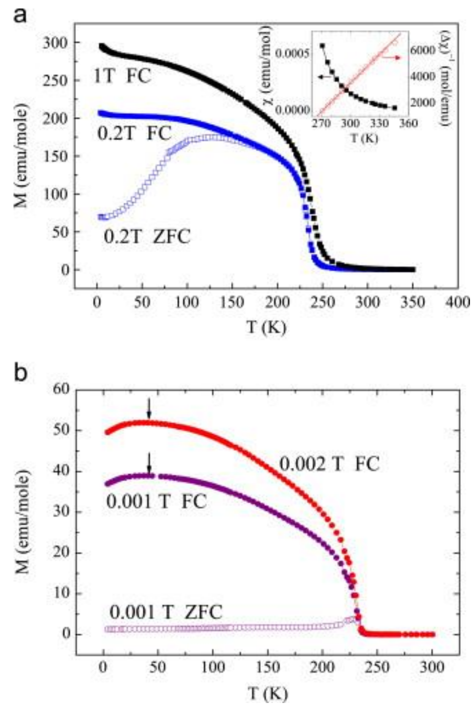

Fig. 2 (Color online.) Temperature dependence of the magnetization M (T) measured under (a) 0.2 T and 1 T; (b) 0.001 T and 0.002 T. The inset of (a) shows <math altimg="si0001.gif" overflow="scroll"> <mi> χ</mi> <mo stretchy="false"> (</mo> <mi> T</mi> ...

Min Ge , Shun Tan , Yuanjie Huang , Lei Zhang , Wei Tong , Li Pi , Yuheng Zhang

Magnetism of insulator Sr2IrO4 with strong spin–orbit coupling

Journal of Magnetism and Magnetic Materials, Volume 345, 2013, 13 - 17

http://dx.doi.org/10.1016/j.jmmm.2013.05.022

Orbital degeneracy and crystal field in Sr_2IrO_4:

- octahedra stretched along z-axis
- **orbital degeneracy is lifted**

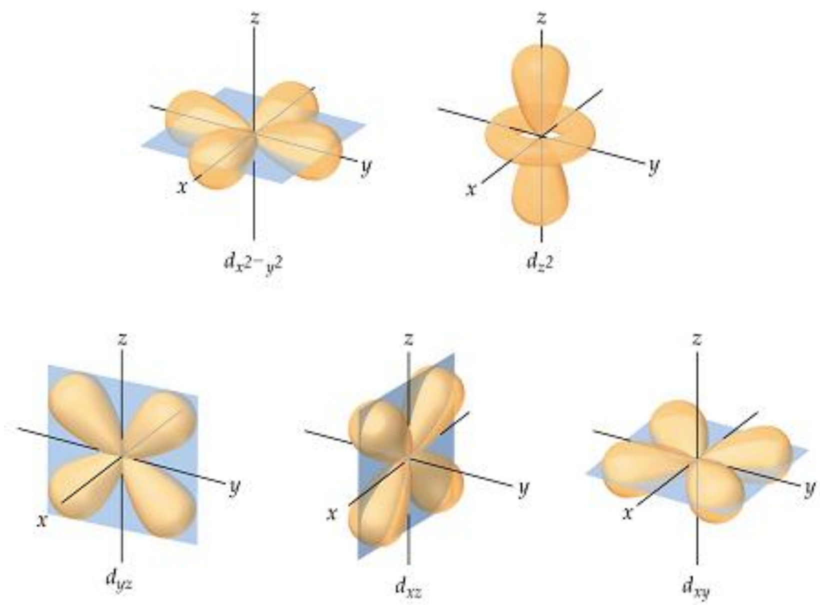

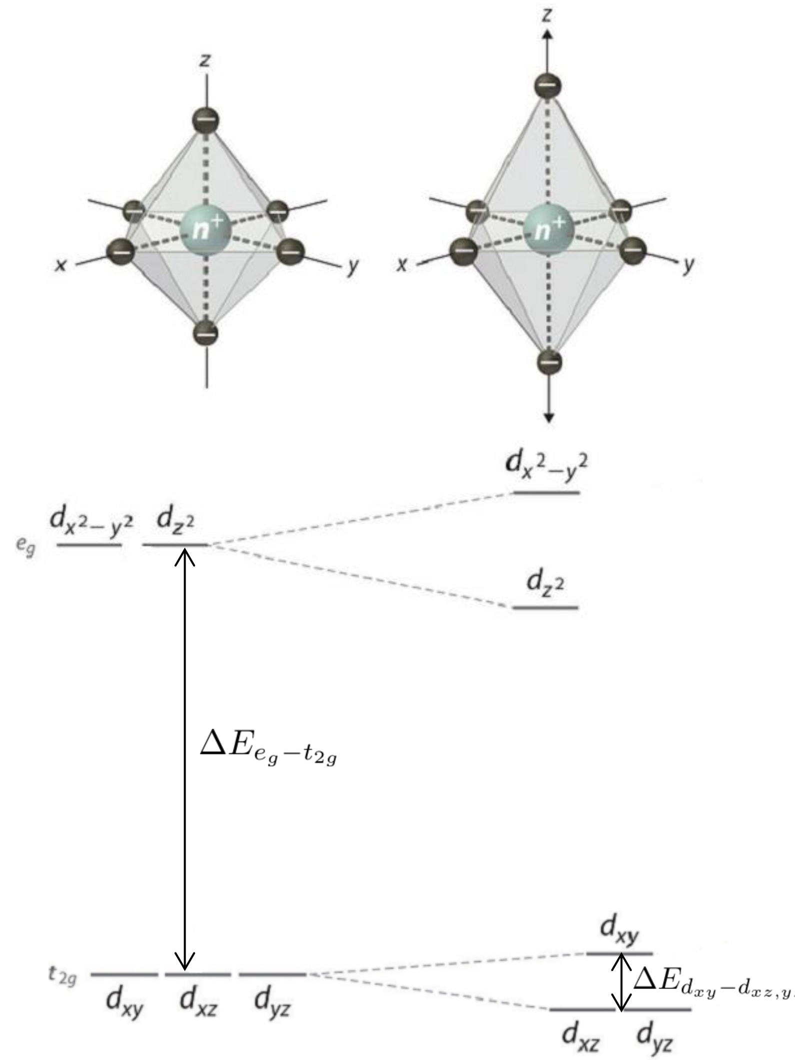

$$\Delta E_{e_g - t_{2g}} \gg \Delta E_{d_{xy} - d_{xz,yz}}$$

$$\Delta E_{e_g - t_{2g}} = 2eV$$

Orbital degeneracy and crystal field in Sr_2IrO_4

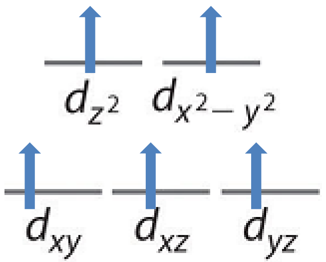

- **assumption of a small CF:**
- Hund´s rule: High spin, S=5/2

- **electron configuration in Sr_2IrO_4:**

large CF $\Delta E_{e_g - t_{2g}} = 2eV$

$\Delta E_{d_{xy} - d_{xz,yz}}$ small:

Hund´s rule broken:

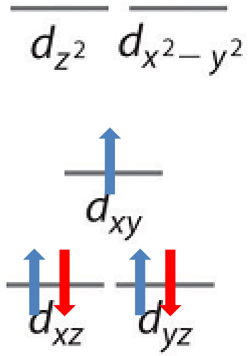

⇨ low spin state (S=1/2), e_g orbitals empty

degenerate t_{2g} orbitals behave like effective p-orbitals with L_{eff}=1

L_{eff}=1:

1) angular part of wave function described by spherical harmonics, Y_{lm} with $Y_{lm} := |m\rangle; \quad l=2$:

- all d-orbitls real $L_z|m\rangle = 0$ for all **individual** d-orbitals:

➢ **orbital momentum is quenched**

2) for degenerate orbitals, orbital momet is partially restored:

a. consider 1 electron in triply degenerate t_{2g} *orbitals:*

➢ **degenerate t_{2g} orbitals behave like effective p-orbitals with L_{eff}=1**

How strong spin-orbit coupling drives a Mott insulating state?

see Board!

The SO-assisted Mott state

- L_{eff}=1 with S=1/2 $\Leftarrow$

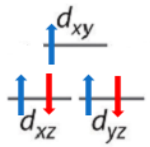

- J_{eff} =1/2 doublet and J_{eff}=3/2 quartet band
- with energy difference ζ_{SO}

B.J. Kim et al. PRL 101 (2008)

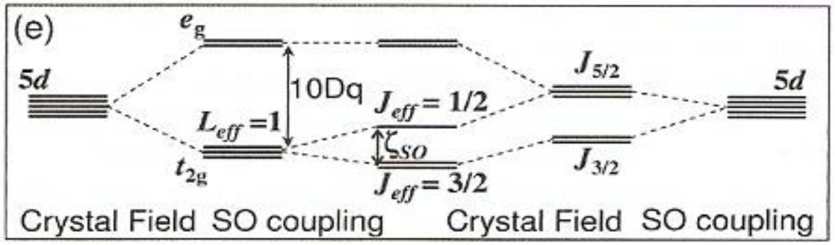

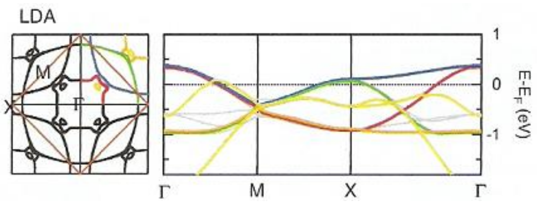

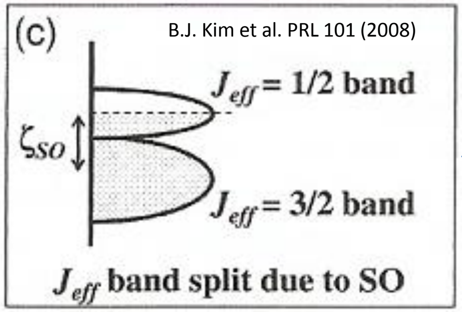

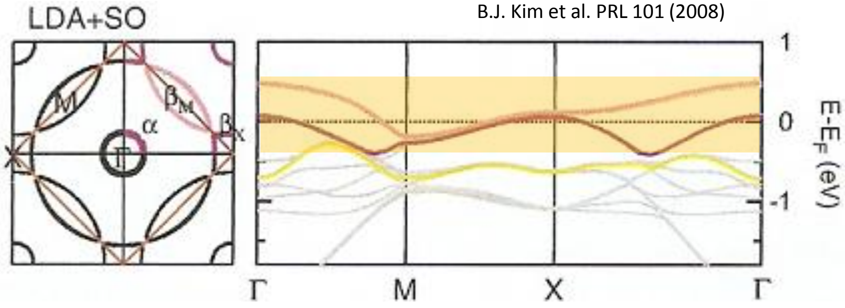

still metallic

$$W_{J_{eff}=1/2} \approx 1eV$$

The SO-assisted Mott state in Sr_2IrO_4

$\boldsymbol{L_{eff}}$=1 with $\boldsymbol{S}$=1/2, → $\boldsymbol{J_{eff}}$ =1/2 doublet and $\boldsymbol{J_{eff}}$=3/2 quartet bands

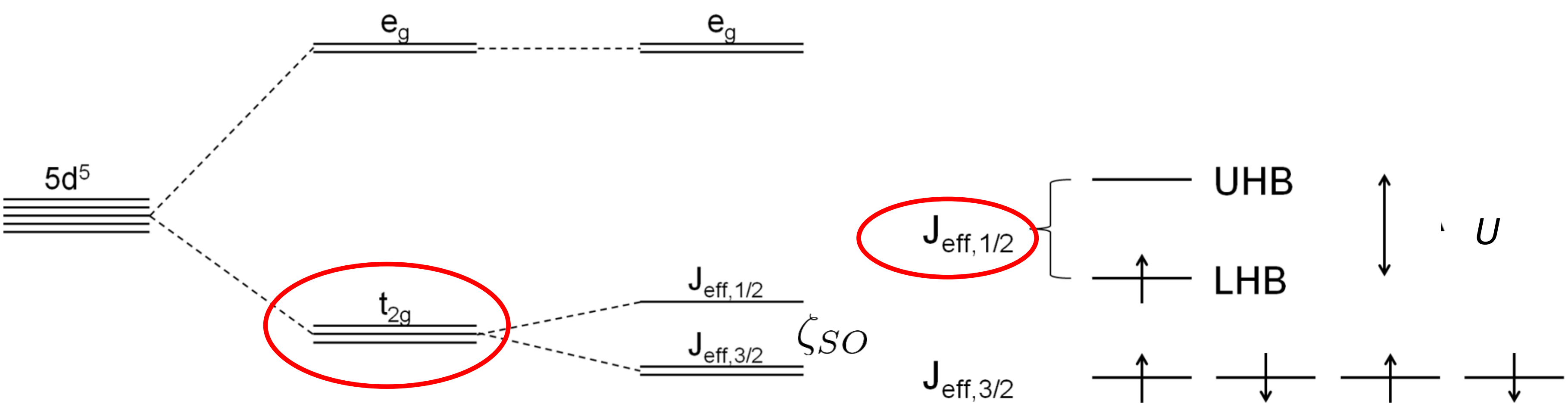

By a strong Spin-Orbit coupling the t_{2g} band splits into effective total angular momentum J_{eff}*=1/2* doublet and J_{eff}*=3/2* quartet bands. Splitting ζ_{SO}

The J_{eff}*=1/2* spin-orbit states form a narrow band so that even small *U* opens a Mott gap, making it a Mott insulator.

narrow J_{eff}=1/2 band with Hubbard U

→ **J_{eff}=1/2 Mott ground state**

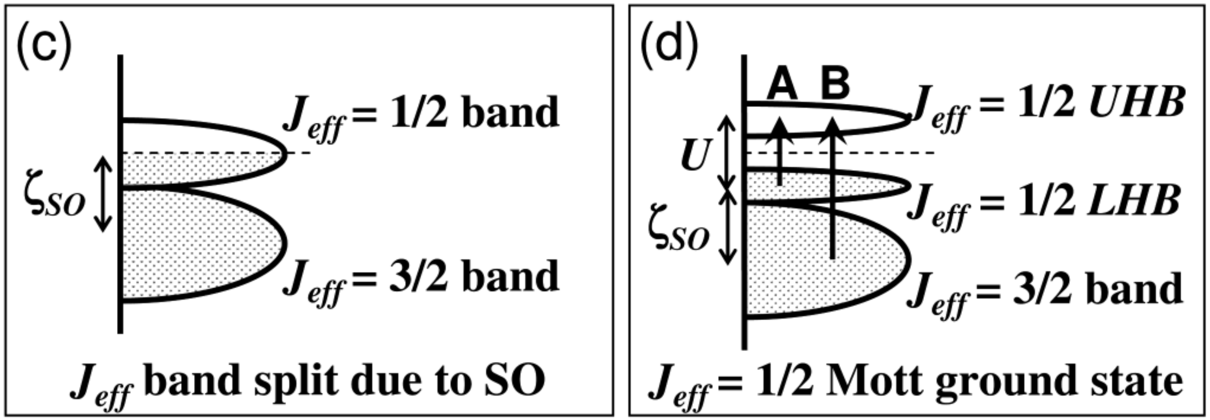

$$U > W_{J_{eff}=1/2}$$

Theory: LDA+SO+U → insulating ground state

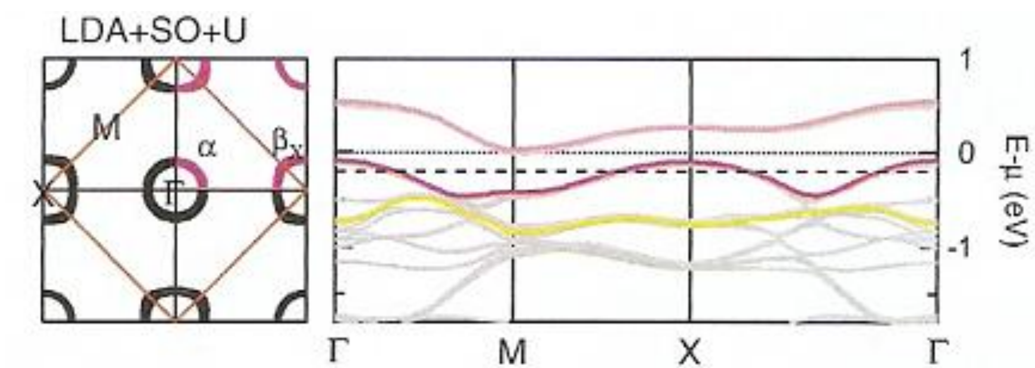

B. J. Kim, PRL 101, 076402 (2008)